BIOCHEMISTRY
### including biophysical chemistry & molecular biology

Recruiting a Silent Partner for Activation of the Protein Kinase SRPK1

Brandon E. Aubol and Joseph A. Adams*

Department of Pharmacology, University of California, San Diego, La Jolla, California 92093-0636, United States

S *Supporting Information*

ABSTRACT: The SRPK family of protein kinases regulates mRNA splicing by phosphorylating an essential group of factors known as SR proteins, so named for a C-terminal domain enriched in arginine–serine dipeptide repeats (RS domains). SRPKs phosphorylate RS domains at numerous sites altering SR protein subcellular localization and splicing function. The RS domains in these splicing factors differ considerably in overall length and dipeptide layout. Despite their importance, little is known about how these diverse RS domains interact with SRPKs and regulate SR protein phosphorylation. We now show that sequences distal to the SRPK1 consensus region in the RS domain of the prototype SR protein SRSF1 are not passive as originally thought but rather play active roles in accelerating phosphorylation rates. Located in the C-terminal end of the RS domain, this nonconsensus region up-regulates rate-limiting ADP release through the nucleotide release factor, a structural module in SRPK1 composed of two noncontiguous sequence elements outside the kinase core domain. The data show that the RS domain in SRSF1 is multifunctional and that sequences once thought to be catalytically silent can be recruited to enhance the efficiency of SR protein phosphorylation.
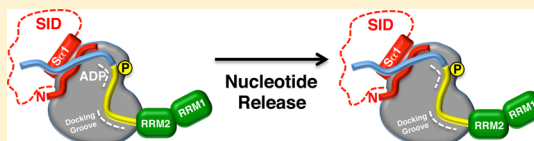
Proteome diversity is regulated in part through the alternative splicing of exons and introns within large precursor mRNA (pre-mRNA) transcripts. The choice of splice-sites critical for cellular function occurs in the spliceosome, a macromolecular assembly of five snRNPs (U1–6) and over 100 protein constituents.[1,2] In the latter category, the SR proteins are essential factors that guide assembly of spliceosomal components from early steps involving splice-site selection to late steps involving the transesterification reactions. SR proteins constitute a group of 12 proteins that are so named owing to a C-terminal domain rich in arginine–serine dipeptide repeats (RS domain).[3] The SRPK family of protein kinases phosphorylates these RS domains at numerous sites, a process that enhances interactions with an SR-specific transporter (TRN-SR) and directs SR proteins from the cytoplasm to the nucleus where they can engage the splicing machinery.[4,5] SRPKs are also associated physically with the spliceosome so they are likely to serve additional, SR-directed functions in the nucleus.[6] Phosphorylation has been shown to regulate interactions of SR proteins with early components of the spliceosome including U1 and U2AF35 that bind near the 5′ and 3′ ends of exon–intron pairs.[7,8] Varying levels of bulk phosphorylation cause changes in gene splicing suggesting that phosphorylation status is linked not only to subcellular localization but also to splice-site choice.[9–11] Despite this precedence, there has been a lack of detail on the connection between region-specific phosphorylation in SR proteins and splicing outcomes. This problem is deeply confounded by the inherent complexity of the RS domains in SR proteins. Both the sizes (~50–300 residues) and arginine–serine contents of RS domains differ significantly, raising the question of how SRPKs recognize and process such a diverse family of SR proteins.

Much of what we know about SR protein phosphorylation has come from studies on SRPK1 and its prototype SR protein substrate SRSF1 (aka ASF/SF2). SRSF1 contains two RNA binding motifs [RRMs] that are essential for the recognition of pre-mRNA. The RS domain of SRSF1 (~50 residues) contains many arginine–serine dipeptides clustered in both short and long repeats (Figure 1A). Footprinting experiments indicate that SRPK1 rapidly phosphorylates the N-terminal serines in the RS domain (RS1) using a directional (C-to-N-terminal) mechanism in which serines are sequentially fed from a docking groove to the active site[12–15] (Figure 1B). Immunocytochemical experiments indicate that phosphorylation of these arginine–serine dipeptides is essential for the SRPK1-dependent transport of SRSF1 to the nucleus.[16] Thus, both in vitro and cell-based analyses define the RS1 segment as both the critical consensus site for SRPK1 phosphorylation and the functional region for kinase-directed SRSF1 transport. Although SRPK1 rapidly phosphorylates RS1, its primary site, it can also modify the shorter arginine–serine dipeptide repeats in RS2 but only at a very slow rate.[12] Detailed kinetic experiments indicate that the rate of RS2 phosphorylation is more than 100-fold slower than that for RS1.[17] In addition to the difficulty of this C-terminal phosphorylation reaction, there is currently no data linking SRPK1-dependent phosphorylation of RS2 with a biological function. The CLK family of nuclear kinases is capable of efficiently phosphorylating RS2, thereby altering the subnuclear localization of SRSF1.[16] However, for cytoplasmic–nuclear localization, the current data suggest that serines in RS2 may serve only a spectator function with regard to SRPK1 phosphorylation activity.
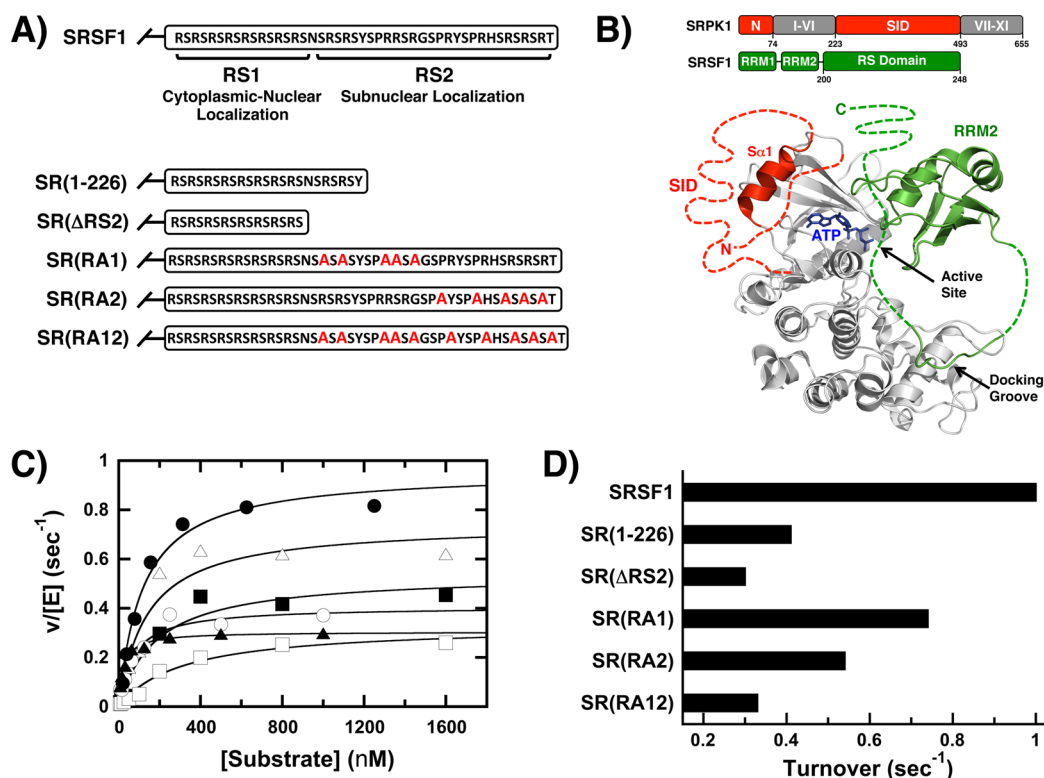
Figure 1. C-terminal residues in the RS domain increase SRSF1 turnover. (A) Wild-type and mutant forms of the SR protein SRSF1. Residues 204–248 of the RS domain are shown, and the RRMs (RRM1 and RRM2) are omitted. (B) Structure of SRPK1 in complex with SRSF1. The two lobes of the kinase domain [subdomains I–VI (N-lobe) and VII–XI (C-lobe)] are shown in gray. SRPK1 lacks its N-terminus (dotted red line) and most of the SID with the exception of helix Sα1 (red). SRSF1 was crystallized without RRM1 and residues 220–248 (RS2). Disordered residues 211–219 (part of RS1) and 197–200 (linker between RRM2 and RS domain) are shown as dotted green lines. Residues 201–210 (N-terminus of RS1) are visible in the docking groove in the C-lobe of the kinase domain. (C) Plot of initial velocity versus SRSF1 (●), SR(1–226) (○), SR(ΔRS2) (▲), SR(RA1) (△), SR(RA2) (■), SR(RA12) (□). Data fits are included in Table 1. (D) Bar graph showing turnover numbers (k_{cat}) for each substrate.

SRPKs represent a highly distinctive family of protein kinases based on unique sequence elements outside the conserved kinase domain. All SRPKs possess an N-terminal extension and a large spacer insert domain (SID) that bifurcates the kinase domain near the interface between the N- and C-lobes (Figure 1B). The SID is similar in size to the kinase domain (~270 aa) and plays an essential role in regulating cytoplasmic–nuclear transport of SRPK1. Although SRPK1 can be found both in the cytoplasm and in the nucleus, removal of the SID causes large movements of the kinase to the nucleus.[18] Epidermal growth factor (EGF) signaling has been shown to regulate this translocation through Akt-induced changes in the binding of several chaperones to the SID.[9,19] Although the SID is mostly unfolded, a small region at the N-terminal edge adopts a helical conformation (Sα1) that interacts with the ATP-binding N-lobe of the kinase domain (Figure 1B). Some recent studies now suggest that this helix may interact with the N-terminus in SRPK1. The SID has been shown to protect backbone amides in the N-terminus from solvent deuterium exchange suggestive of a physical interaction.[20] Furthermore, it has been shown that this coupling of sequences in the N-terminus and SID is important for SRPK1 activity regulation. Deletion analyses indicate that helix Sα1 and the N-terminus work cooperatively to facilitate rapid SRSF1 phosphorylation through an increase in ADP release (10-fold), the rate-limiting step for RS domain phosphorylation.[21] Overall, these two regions, external to the kinase domain and separated in primary structure, act as a

nucleotide release factor [NRF] that up-regulates SRSF1 phosphorylation.

Despite many advances in understanding the mechanism of SR protein phosphorylation, very little is known about how these lengthy RS domains interact with SRPKs. The current X-ray structure for SRPK1 and its substrate SRSF1 lacks electron density for RS1 residues in the active site and contains no RS2 sequences (Figure 1B). Only a short 10-residue stretch of RS1 (residues 201–210) is visible in a docking groove in the large C-lobe of the kinase domain. Whether residues outside RS1 make contacts with the kinase and impact SR protein phosphorylation is not known. To address this, we studied the effects of deletion and block mutations on the kinetic mechanism of RS1 phosphorylation. Using rapid quench flow and viscosometric experiments, we found that RS2 enhances SRSF1 phosphorylation by up-regulating ADP dissociation rates. The phosphorylation of an SRSF1 deletion construct lacking RS2 is increased by the addition of an RS2 peptide, suggesting that the C-terminal end of the RS domain binds outside the active site. RS2-dependent activation of substrate phosphorylation occurs only in the presence of a functioning NRF. The combined data indicate that the RS2 segment is not a passive element in the RS domain as once thought but rather plays an active role in controlling SR protein phosphorylation. Although the NRF asserts a basal level of activation through enhancements in ADP release, full activation is achieved through an NRF–RS2 connection. These studies help clarify how regions in the RS domain that are not part of the

immediate consensus sequence and not characterized by structural analyses interact with SRPK1. These new findings raise the possibility that other SR proteins with much larger and more diverse RS domains could also interact with the NRF of SRPK1 regulating consensus arginine−serine phosphorylation sites.

■ MATERIAL AND METHODS

Materials. Adenosine triphosphate (ATP), 3-(*N*-morpholino)propanesulfonic acid (Mops), tris(hydroxymethyl) aminomethane (Tris), MgCl₂, NaCl, EDTA, glycerol, sucrose, acetic acid, Phenix imaging film, BSA, Whatman P81 grade filter paper, and liquid scintillant were obtained from Fisher Scientific. [γ-³²P]ATP was obtained from NEN Products, a division of PerkinElmer Life Sciences.

Expression and Purification of Recombinant Proteins. All wild-type and deletion forms of SRPK1 were expressed from a pRSETb vector containing a 6xHis Tag at the N terminus.[22] SRPK1(ΔN), SRPK1(ΔS), SRPK1(ΔS$_{INT}$), and SRPK1-(ΔSα1) were made by deleting residues 1−73, 224−492, 248−483, and 224−249, respectively, and were previously described.[20,21] SRSF1 was expressed from a pET19b vector containing a 10xHis Tag at the N terminus.[15] All charge-to-alanine mutations in SRSF1 were generated by sequential polymerase chain reactions using the QuikChange mutagenesis kit and relevant primers (Stratagene, La Jolla, CA) and were previously described.[23] SR(ΔRS2) was expressed in pET28a vector containing a C-terminal His tag and was previously described.[12] The plasmids for SRSF1 and SRPK1 were transformed into the BL21 (DE3) *Escherichia coli* strain, and the cells were then grown at 37 °C in LB broth supplemented with 100 mg/mL ampicillin or 50 mg/mL kanamycin depending on the type of plasmid vector. Protein expression was induced with 0.4 mM IPTG at room temperature for 5 h for SRSF1 and 12 h for SRPK constructs. All SRPK1 constructs were purified by Ni-resin affinity chromatography using a published procedure.[24] SRSF1 was refolded and purified using a previously published protocol.[14]

Phosphorylation Reactions. The phosphorylation of wild-type and mutant forms of SRSF1 by wild-type and mutant forms of SRPK1 were carried out in the presence of 100 mM Mops (pH 7.4), 10 mM free Mg²⁺, and 5 mg/mL of BSA at 23 °C according to previously published procedures.[14] All reactions were initiated with the addition of enzyme and were carried out in a total reaction volume of 10 μL and quenched with 10 μL of SDS-PAGE loading buffer. Competition reactions were carried out using fixed amounts of SR(ΔRS2) or SRSF1 (50 nM) as a substrate and varying concentrations of the competitor SR(RS2). Phosphorylated SR protein was separated from unreacted [γ-³²P]ATP by loading the quenched reaction on an SDS-PAGE gel (16%) and running at 170 V for 1 h. Protein bands corresponding to phosphorylated SR protein were cut from the dried SDS-PAGE gel and quantitated on the ³²P channel in liquid scintillant. The total amount of phosphoproduct was then determined by considering the specific activity (cpm) of the reaction mixture and the background retention of [γ-³²P]ATP in the absence of enzyme.

Rapid Quench Flow Experiments. Phosphorylation of SRSF1 and SR(ΔRS2) by SRPK1 was monitored using a KinTek Corporation model RGF-3 quench flow apparatus. The apparatus consists of three syringes driven by a stepping motor. Typical experiments were performed by mixing equal volumes

of the SRPK1−SRSF1 complex in one reaction loop and ³²P-ATP (5000−15000 cpm/pmol) in the second reaction loop in 100 mM Mops (pH 7.4), 10 mM free Mg²⁺, and 5 mg/mL BSA. All enzyme and ligand concentrations are those in the mixing chamber unless otherwise noted. The reactions were quenched with 30% acetic acid in the third syringe, and phosphorylated SRSF1 was separated from unreacted ATP by a filter-binding assay where a portion of each quenched reaction (50 μL) was spotted onto a phosphocellulose filter disk and was washed three times with 0.5% phosphoric acid.[17] The filter disks were rinsed with acetone, dried, and counted on the ³²P channel in liquid scintillant. The total amount of phosphate incorporated into the substrate was then determined as described above. Full retention of the phosphorylated product on the filters was confirmed by running quenched reaction samples on SDS-PAGE and counting the bands.

Viscosity Experiments. SR(ΔRS2) phosphorylation was monitored using the filter binding assay as described above in the presence of 0−30% sucrose. The relative solvent viscosity (η^{rel}) of the buffer (100 mM Mops, pH 7.4) containing 0−30% sucrose was measured using an Ostwald viscometer and a previously published protocol.[25] Values of 1.44, 1.83, 2.32, and 3.43 for η^{rel} were measured for buffers containing 10%, 20%, 25%, and 30% sucrose at 23 °C, respectively.

Data Analysis. The amount of phosphoproduct was determined from the specific activity of ³²P-ATP and the cpm of excised bands corrected for background. The initial velocity data were fit to the Michaelis−Menten equation to obtain K_m and V_{max}. The V_{max} values were converted to k_{cat} using the total enzyme concentration determined from a Bradford assay ($k_{cat} = V_{max}/E_{tot}$). In pre-steady-state kinetic experiments, the reaction product ([P]) as a function of time was fit to eq 1:

$$[P] = \alpha[1 - \exp(-k_b t)] + k_L E_o t \tag{1}$$

where α, k_b, k_L, and E_o are the amplitude of the "burst" phase, the rate constant for the "burst" phase, the rate constant for the linear phase, and the total enzyme concentration, respectively. The dissociation constant (K_I) for SR(RS2) to SRPK1 using fixed amounts of SRSF1 was measured using eq 2:

$$\frac{v_i}{v_o} = \frac{K_I\left(1 + \frac{[S]}{K_{SR}}\right)}{[I] + K_I\left(1 + \frac{[S]}{K_{SR}}\right)} \tag{2}$$

where v_i/v_o is the relative initial velocity (ratio of v in the presence and absence of inhibitor), K_{SR} is the K_m for SRSF1, and [I] is the SR(RS2) concentration. The activation constant (K_A) for SR(RS2) to SRPK1 using fixed amounts of SR(ΔRS2) ([S]) was determined using eq 3:

$$\frac{v_i}{v_o} = \frac{a + b[A]}{a + c[A] + K_{SR}[A]^2} \tag{3}$$

where

$$a = K_A K_I([S] + K_{SR})$$

$$b = \gamma K_I([S] + K_{SR})$$

$$c = K_I([S] + K_{SR}) + K_{SR}K_A$$

γ is the change in k_{cat} for SR(ΔRS2) phosphorylation in the presence of SR(RS2) in the activation site, K_{SR} is the K_m for SR(ΔRS2), and [A] is the concentration of SR(RS2).

■ RESULTS

C-Terminal Sequences in the RS Domain Regulate SRSF1 Turnover. Although SRPK1 rapidly phosphorylates a patch of N-terminal serines (RS1) in SRSF1 (Figure 1A), very little is known about how or whether the full RS domain interacts with the kinase. Large portions of the RS domain are not part of the cocrystal or have poor electron density (Figure 1B). To determine whether residues in the RS2 segment play any role in controlling RS1 phosphorylation by SRPK1, we studied the steady-state kinetic properties of five forms of SRSF1 that contain modifications to RS2 (Figure 1A). All mutants displayed reduced maximal velocities relative to the wild-type SR protein (Figure 1C). Deletions in the RS2 segment [SR(ΔRS2) and SR(1−226)] resulted in about 2−3-fold reductions in k_{cat} compared with that for the wild-type substrate (Figure 1D and Table 1). Although the substrate K_m

Table 1. Steady-State Kinetic Parameters for Wild-Type and Mutant Forms of SRSF1

substrate	enzyme	k_{cat} (s^{-1})	K_{SR} (nM)	K_{ATP} (μM)
SRSF1	SRPK1	1.0 ± 0.05	110 ± 20	11 ± 2
SR(1−226)	SRPK1	0.4 ± 0.04	70 ± 17	
SR(ΔRS2)	SRPK1	0.30 ± 0.01	25 ± 5	16 ± 2
SR(ΔRS2)	SRPK1(ΔN)	0.10 ± 0.01	110 ± 39	
SR(ΔRS2)	SRPK1(ΔS)	0.13 ± 0.01	30 ± 13	9 ± 3
SR(RA1)	SRPK1	0.74 ± 0.06	140 ± 40	
SR(RA2)	SRPK1	0.54 ± 0.06	180 ± 70	
SR(RA12)	SRPK1	0.33 ± 0.02	300 ± 70	

(K_{SR}) was mostly unaffected for SR(1−226), that for SR(ΔRS2) showed a 4-fold decrease (Table 1). Removal of RS2 sequences does not affect the apparent affinity of ATP (Table 1). Based on MALDI-TOF analyses, both deletion mutants displayed reductions in total phosphoryl content that are consistent with the reduced numbers of serines (Suppl. Figure S1, Supporting Information). To evaluate whether the reductions in k_{cat} are due to electrostatic residues, we made three arginine-to-alanine block mutations in RS2. Removing all arginines in SR(RA12) leads to a 3-fold reduction in k_{cat} similar to that for SR(ΔRS2) suggesting that charges in RS2 are important for controlling substrate turnover (Figure 1D and Table 1). Partial removal of arginines in SR(RA1) and SR(RA2) leads to intermediate effects on k_{cat} suggesting that numerous positive charges throughout RS2 are associated with regulating substrate turnover. The phosphoryl contents of the arginine-to-alanine mutants were similar to that for SRSF1 (Suppl. Figure S1, Supporting Information). Overall, the kinetic data indicate that residues outside RS1 control the maximum rate of SRSF1 phosphorylation.

RS2 Up-Regulates SRSF1 Phosphorylation by Accelerating ADP Release. In a prior study, we showed that SRSF1 phosphorylation by SRPK1 is limited by ADP release.[17] We also showed that the RRMs play no role in controlling this rate-limiting step suggesting that any potential regulation through the substrate is likely to come from within the RS domain.[17] To determine whether sequences outside RS1 affect product release, we initially assessed the role of viscosogenic agents on substrate phosphorylation.[17,25,26] For these studies, we focused on SR(ΔRS2) since it displayed the largest decrease in k_{cat} (Figure 1D). In plots of initial velocity versus ATP using saturating SR(ΔRS2), we found that increasing glycerol leads

to decreases in k_{cat} and k_{cat}/K_{ATP} (Figure 2A). The data are interpreted using Scheme 1 where k_1 is the ATP association step, k_2 is the viscosity-independent phosphoryl transfer step, and k_3 is the viscosity-dependent, net rate constant for product release. A slope of one is obtained in plots of relative k_{cat} versus relative solvent viscosity implying that k_2 is at least 3 s^{-1} and is not rate-limiting for this parameter (Figure 2B and Table 2). In contrast, this maximum slope implies that k_3 is fully rate-limiting for k_{cat}. We observed a slope close to one for k_{cat}/K_{ATP} indicating that k_1 limits this kinetic parameter (Figure 2B and Table 2). To further support these findings, we performed pre-steady-state kinetic experiments and showed that SR(ΔRS2) phosphorylation observes "burst" kinetics similar to that for the wild-type substrate and consistent with a fast, observed rate of phosphoryl transfer ($k_b \approx 10-20$ s^{-1}) in the active site (Figure 2C). Although the observed errors preclude a detailed comparison, the data show definitively that the phosphoryl transfer step is not rate-limiting for SRSF1 and SR(ΔRS2). In contrast to phosphoryl transfer, the linear phase rate constant (k_L) for SRSF1 phosphorylation is very well-defined and is 3-fold faster than that for SR(ΔRS2) in keeping with the steady-state kinetic results (Table 1). Overall, these data imply that the decline in k_{cat} for SR(ΔRS2) is not the result of slow phosphoryl transfer but is rather consistent with a reduction in the release rate for one or both of the reaction products [ADP or phospho-SR(ΔRS2)].

To determine whether the rate-limiting, viscosity-dependent step for SR(ΔRS2) phosphorylation is ADP release, we employed catalytic trapping (C$_{AT}$T$_{RAP}$) methods.[27,28] In the C$_{AT}$T$_{RAP}$ experiment, SRPK1 is pre-equilibrated with saturating ADP and SR(ΔRS2) and then mixed with excess ATP in the rapid quench flow machine (Scheme 2). We found that the "burst" phase disappeared in the presence of ADP and was replaced by a small lag prior to the linear, steady-state phase (Figure 2D). The observed rate of the linear phase in the absence and presence of ADP is the same implying that sufficient ATP is used to trap the kinase and prevent ADP rebinding. The data were initially simulated in the absence of ADP using Scheme 2 and the program DynaFit[29] to obtain rate constants for the phosphoryl transfer step (k_2) of 18 s^{-1} and net product release (k_3) of 0.3 s^{-1} (Figure 2D and Table 2). For these simulations, we used k_{cat}/K_{ATP} as the association rate constant for ATP (k_1) based on the viscosity data. In the presence of ADP pre-equilibration, the data were simulated with these fixed rate constants (k_1, k_2, and k_3) to obtain the dissociation rate constant for ADP (k_{off}) of 0.3 s^{-1} (Figure 2D and Table 2). We could show in comparative simulations that the C$_{AT}$T$_{RAP}$ method is highly sensitive to very small differences in k_{off}. In Figure 2D, we present additional simulations where k_{off} is elevated by 20−100%. The data become progressively sigmoidal as k_{off} increases and even at 0.37 s^{-1} poorly simulate the observed kinetic transient. These findings show that the rate-limiting step for SR(ΔRS2) turnover is ADP rather than pSRSF1 release and that the RS2 segment controls this step. Furthermore, these experiments reveal that RS2 plays a positive role in regulating the rate-limiting step for RS1 phosphorylation.

RS2 Activates SRPK1 by Binding Outside the Active Site. Owing to its impact on catalysis, we speculated that the RS2 segment might bind somewhere outside the active site providing a mechanism for SRSF1 phosphorylation enhancement. To address this possibility, we expressed a C-terminal His-tagged form of the substrate that contains only RS2
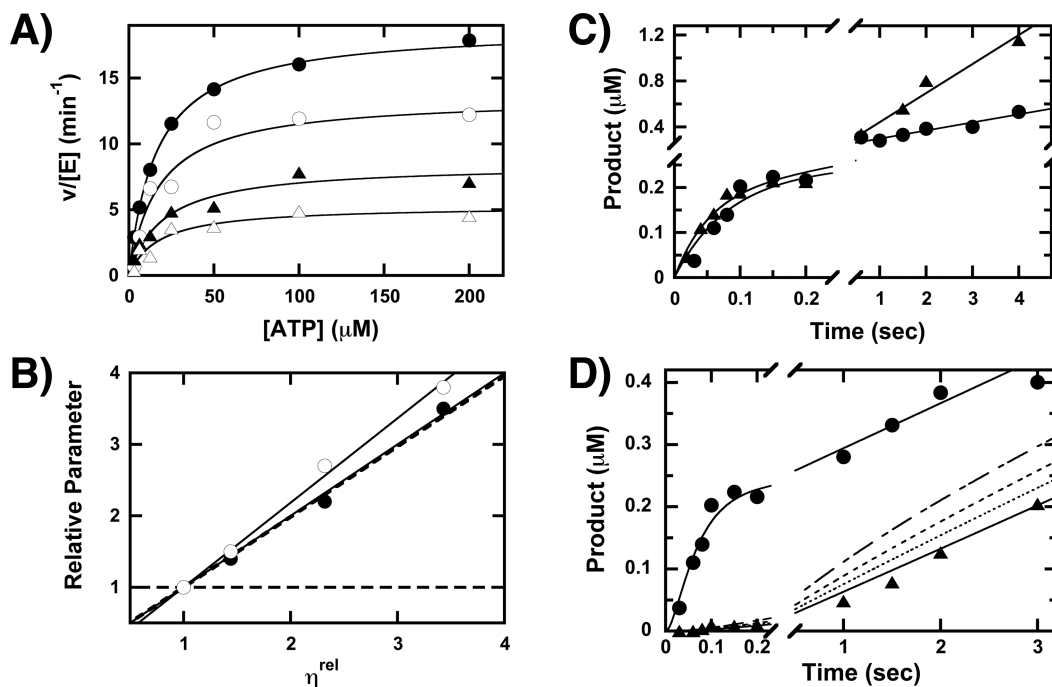
Figure 2. RS2 controls the release rate for ADP. (A) Glycerol effects on SR(ΔRS2) phosphorylation. Plots of initial velocity versus ATP at 0% (●), 10% (○), 25% (▲), and 30% (△) sucrose. (B) Relative k_{cat} and k_{cat}/K_{ATP} (ratios in the absence and presence of sucrose) versus relative solvent viscosity for the data in panel A. Slopes of 1.0 and 1.2 are obtained for relative k_{cat} and k_{cat}/K_{ATP}. Dotted lines represent theoretical slope values of 0 and 1. (C) Pre-steady-state kinetic transients for SR(ΔRS2) (●) and SRSF1 (▲) phosphorylation. SRPK1 (0.25 μM) is mixed with SR protein (0.5 μM) and ATP (600 μM) in the rapid quench flow machine. The data are fit to eq 1 to obtain values of 0.23 ± 0.02 μM, 12 ± 3 s^{-1}, and 0.28 ± 0.01 s^{-1} for α, k_b, and k_L, respectively, for SR(ΔRS2) and values of 0.22 ± 0.03 μM, 19 ± 8 s^{-1}, and 1.0 ± 0.01 s^{-1} for α, k_b, and k_L, respectively, for SRSF1. (D) $C_{AT}T_{RAP}$ experiment. SRPK1 is preincubated with SR(ΔRS2) in the absence (●) and presence (▲) of 120 μM ADP in one syringe (60 μM in reaction) of the rapid quench machine and then mixed with ATP (600 μM in reaction) to start the reaction. The data in panel D are simulated using DynaFit[29] and the mechanism in Scheme 2 to obtain values of 0.3 s^{-1}, 18 s^{-1}, and 0.3 s^{-1} for k_{off}, k_2, and k_3, respectively (solid lines). A value of 19 mM^{-1} s^{-1} for the k_1 was used for both simulations. Additional simulations in the presence of ADP are displayed in which k_{off} is increased to values of 0.37 s^{-1} (···), 0.45 s^{-1} (– – –), and 0.6 s^{-1} (— · —).
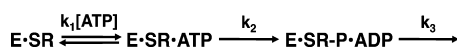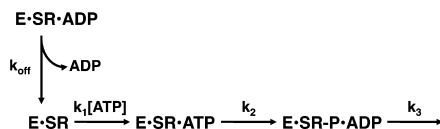
Scheme 1

Table 2. Values of Individual Steps in Schemes 1 and 2 for SRSF1 and SR(ΔRS2) Phosphorylation Using Viscosity and $C_{AT}T_{RAP}$ Methods

substrate	method	k_1 (mM^{-1} s^{-1})	k_2 (s^{-1})	k_3 (s^{-1})	k_{off} (s^{-1})
SRSF1	viscosity	91	$\geq 10^a$	1.0^a	b
SRSF1	$C_{AT}T_{RAP}$	b	30^a	1.0^a	1.1^a
SR(ΔRS2)	viscosity	19	≥ 3	0.3	b
SR(ΔRS2)	$C_{AT}T_{RAP}$	b	18	0.3	0.3

^{a}Data were taken from ref 17. ^{b}Not determined.

Scheme 2

residues [SR(RS2)] (Figure 3A). We showed that SR(RS2) is a substrate for SRPK1 displaying a K_{SR} of 340 nM, a value about 3-fold higher than that for the full-length substrate (Figure 3B). To estimate its true affinity, we performed a competition experiment in which increasing amounts of SR(RS2) are added to SRPK1 in the presence of a fixed amount of full-length

SRSF1.[23] Owing to differences in substrate sizes, SRSF1 phosphorylation can be monitored independently by SDS-PAGE and SR(RS2) can then be treated as a reversible inhibitor in this experiment.[12,23,30] As expected, increasing SR(RS2) decreased the relative initial velocity for SRSF1 phosphorylation consistent with active-site-directed inhibition (Figure 2C). The data were fit to eq 2 using the K_{SR} for SRSF1 to obtain a K_I of 200 nM for SR(RS2). In prior experiments, we showed that the K_I value for SRSF1 is about 100 nM.[23] These findings indicate that SR(RS2) is a substrate for SRPK1 although it displays somewhat weaker affinity for the active site of SRPK1 compared with SRSF1.

When the competition experiment was performed using SR(ΔRS2) as the fixed substrate rather than the full-length SRSF1, a significant departure in the inhibition curve was detected. Surprisingly, catalytic activation was observed at lower SR(RS2) concentrations (50–300 nM) prior to inhibition at higher concentrations (Figure 3C). These results are consistent with a two-site mechanism in which one molecule of SR(RS2) freely binds outside the active site causing activation of SR(ΔRS2) phosphorylation and a second molecule binds in the active site causing inhibition (Scheme 3). To ensure that activation occurs by discretely enhancing turnover, we showed that a low, fixed amount of SR(RS2) (200 nM) increased k_{cat} (~4-fold) without affecting K_{SR} (Figure 3D). Thus, adding the RS2 fragment back to the phosphorylation reaction with SR(ΔRS2) raises k_{cat} to a level similar to that for the full-length SR protein (Table 1). This not only supports the activation
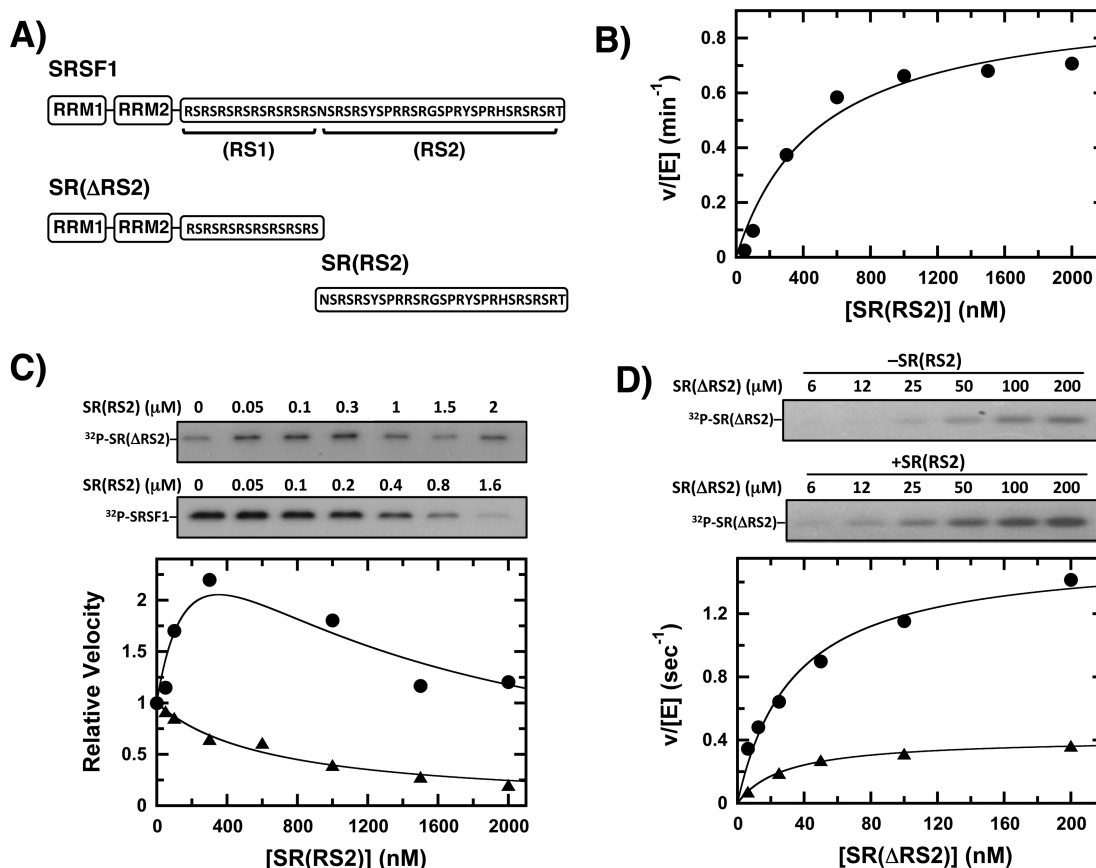
Figure 3. RS2 activates SRPK1 by binding outside the active site. (A) SRSF1 constructs. (B) SR(RS2) is a substrate for SRPK1. Initial velocity data for SR(RS2) phosphorylation are collected using 5 μM ATP and fit to K_{SR} and k_{cat} values of 340 $\pm$ 100 nM and 0.9 $\pm$ 0.1 min^{-1}. (C) Competition with SR(RS2). The relative initial velocities for the phosphorylation of 50 nM SRSF1 ($\blacktriangle$) or SR(ΔRS2) ($\bullet$) are monitored using 5 μM ATP and varying amounts of SR(RS2) (0−2000 nM). For SRSF1, the data are fit to eq 2 to obtain a K_I of 200 $\pm$ 20 nM for SR(RS2) using a fixed value for K_{SR} of 110 nM (Table 1). For SR(ΔRS2) phosphorylation, the data are fit to eq 3 to obtain K_A of 330 $\pm$ 70 nM, K_I of 320 $\pm$ 90 nM, and γ of 5 $\pm$ 0.8 for SR(RS2) using a fixed value for K_{SR} (25 nM). (D) Initial velocity kinetics for SR(ΔRS2) phosphorylation in the absence ($\blacktriangle$) and presence ($\bullet$) of 200 nM SR(RS2). Values for k_{cat} and K_{SR} are 0.33 $\pm$ 0.05 s^{-1} and 30 $\pm$ 9 nM in the absence and 1.3 $\pm$ 0.21 s^{-1} and 28 $\pm$ 11 nM in the presence of SR(RS2) and 100 μM ATP.
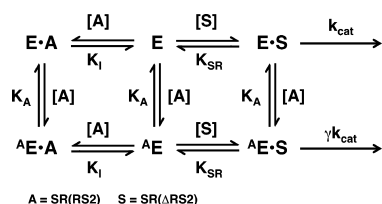
Scheme 3

data in Figure 3C but also demonstrates that SR(RS2) and SR(ΔRS2) do not influence each other's binding. Using the mechanism in Scheme 3 and eq 3, we can quantitatively assess both the activation and inhibition of SR(ΔRS2) phosphorylation by RS2 (Figure 3C). By inserting K_{SR} for SR(219) (Table 1) into eq 3, we can establish the binding constant for SR(RS2) to the activating (K_A = 330 nM) and inhibitory sites (K_I = 320 nM). Although SR(RS2) binds equivalently to both sites, strong activation is observed at low concentrations since the active site is occupied by SR(ΔRS2) whereas the activating site is free using this truncated substrate. Finally, this analytical solution to the data also implies that SR(RS2) increases k_{cat} by about 5-fold (γ), a value in line with the observed effects in plots of velocity versus substrate (Figure 3D). Overall, these

data indicate that in addition to binding in the active site, RS2 can bind outside the active site enhancing substrate turnover.

RS2-Dependent Activation Is Mediated through Both the N-Terminus and SID. To establish whether sequences inside or outside the kinase domain are important for RS2-dependent activation, we investigated how SR(RS2) affects the phosphorylation of SR(ΔRS2) using several truncated forms of SRPK1. In these studies, we expressed and purified two kinase versions that lack either the N-terminus [SRPK1(ΔN)] or the SID [SRPK1(ΔS)] (Figure 4A). While SR(RS2) is a substrate for both kinases, the binding affinity is reduced compared with the wild-type kinase since we were unable to saturate the kinases in plots of initial velocity versus substrate (Figure 4B). In comparison, K_{SR} for SR(ΔRS2) to SRPK1(ΔS) was unaffected and only 4-fold higher for SRPK1(ΔN) compared with the wild-type kinase (Table 1). Using fixed amounts of SR(ΔRS2), we found that the addition of SR(RS2) to SRPK1(ΔN) or SRPK1(ΔS), unlike the wild-type kinase, caused no activation of SR(ΔRS2) phosphorylation (Figure 4C). SR(RS2) caused some inhibition at higher concentrations using SRPK1(ΔS) whereas none was observed with SRPK1-(ΔN) within the detection limits of the experiment. Using K_{SR} for SR(ΔRS2) (Table 1) and eq 2 we can estimate a K_I of 1300 nM for SR(RS2) indicating that removal of the entire SID
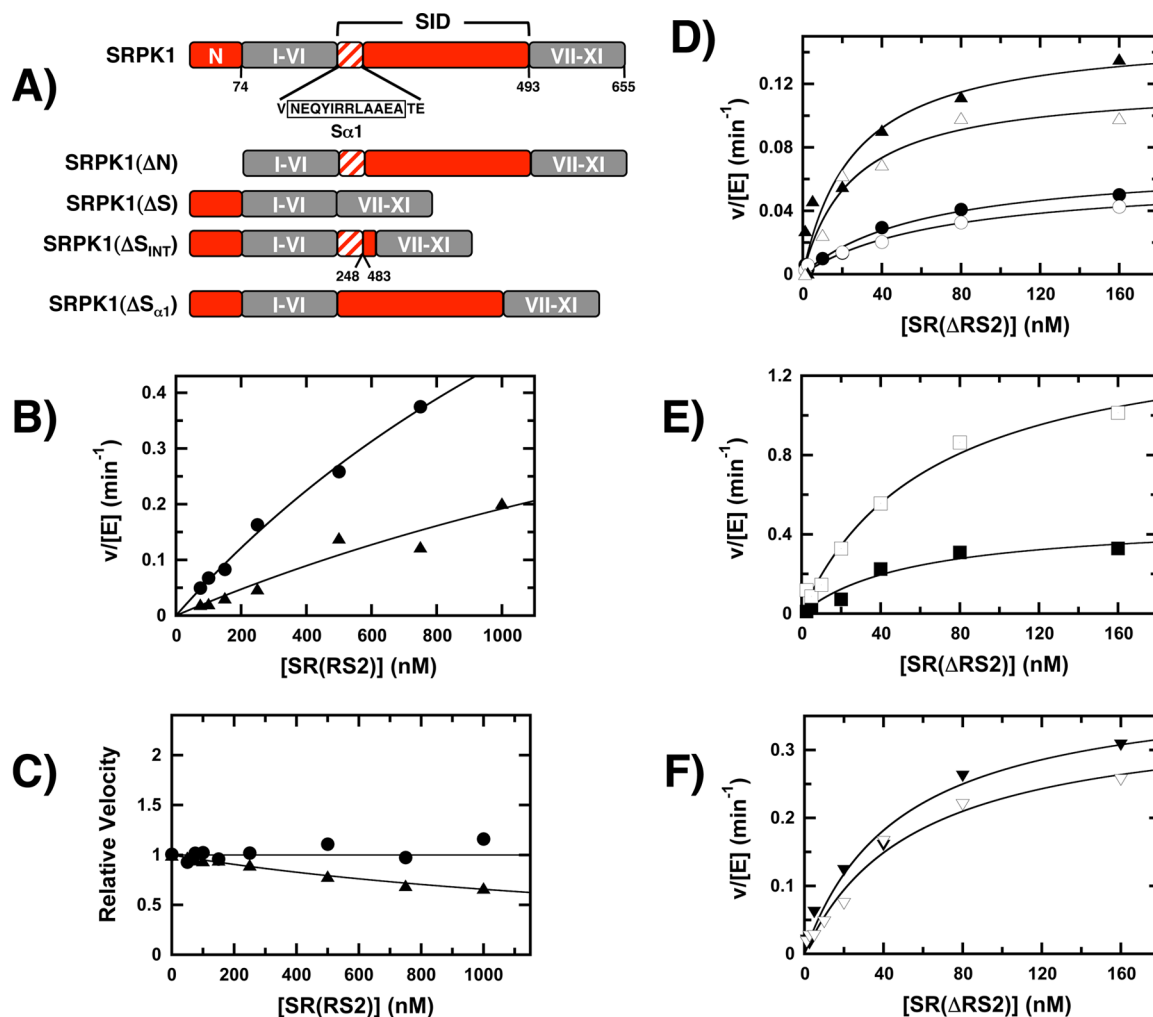
Figure 4. Nucleotide release sequences regulate RS2-dependent activation of SRPK1. (A) SRPK1 deletion constructs. Helix Sα1 in the SID is shown in striped red. (B) SR(RS2) is a substrate for SRPK1(ΔN) (▲) and SRPK1(ΔS) (●). Initial velocity data are collected using 5 μM ATP and fit to a k_{cat}/K_{SR} value of 0.66 ± 0.05 μM^{-1} min^{-1} for SRPK1(ΔS) and 0.25 ± 0.07 μM^{-1}min^{-1} for SRPK1(ΔN). (C) Competition data. The relative initial velocities for SR(ΔRS2) phosphorylation using SRPK1(ΔS) (▲) and SRPK1(ΔN) (●) are plotted as a function of SR(RS2). The data for SRPK1(ΔS) were fit to eq 2 using a K_{SR} of 110 nM to obtain a K_I of 1300 ± 100 nM. (D–F) Plots of initial velocity for SR(ΔRS2) phosphorylation using SRPK1(ΔN) (▲,△), SRPK1(ΔS) (●,○), SRPK1(ΔS$_{INT}$) (■,□), and SRPK1(ΔSα1) (▼,▽) in the absence (filled symbols) and presence (open symbols) of 200 nM SR(RS2). The kinetic parameters are displayed in Table 3

weakens affinity in the active site. Overall, these findings suggest that sequences in both the SID and the N-terminus are critical for RS2-dependent enhancements in SRSF1 turnover.

Nucleotide Release Factor Enables RS2-Dependent Activation. In a previous study, we showed that the N-terminus and a helix (Sα1) at the N-terminal edge of the SID (Figure 1B) act together as a nucleotide release factor [NRF] enhancing SR protein phosphorylation by causing a 10-fold increase in the ADP dissociation rate.[21] To evaluate whether the RS2 segment functions as a molecular trigger for activation through the NRF or possibly through other sequences in the SID, we investigated SR(RS2)-dependent changes in the phosphorylation of SR(ΔRS2) using several truncated forms of SRPK1 (Figure 4A). We initially showed that SR(RS2) did not increase the maximal velocity of SRPK1(ΔN) or SRPK1(ΔS) consistent with the idea that RS2 enhances catalysis through sequences in the N-terminus and SID (Figure 4D and Table 2). A small level of inhibition was observed for SRPK1(ΔN) suggesting that some SR(RS2) is occupying the active site at these levels. We next wished to assess whether

sequences in the SID that are not part of helix Sα1 play a role in controlling SRPK1 activation. SRPK1(ΔS$_{INT}$) removes the majority of the residues in the SID except for those corresponding to helix Sα1 and a short segment that serves as a linker between the helix and the C-terminal lobe of the kinase (Figure 4A). The addition of SR(RS2) increased k_{cat} for SR(ΔRS2) phosphorylation by about 4-fold, a level similar to that for the wild-type SR protein (Figure 4E and Table 3). To confirm that helix Sα1 is essential for the activation process, we studied a kinase form [SRPK1(ΔSα1)] lacking only residues in this helix (Figure 4A). The addition of SR(RS2) did not increase k_{cat} for SR(ΔRS2) phosphorylation but instead caused a small amount of inhibition (Figure 4F and Table 3). Taken together, these data imply that RS2 sequences enhance SR protein phosphorylation through the N-terminus and helix Sα1 in the SID, both core elements of the NRF.

■ DISCUSSION

The RS domains of SR proteins differ substantially in overall length (~50–300 residues) and arginine–serine content.

Table 3. Steady-State Kinetic Parameters for SR(ΔRS2) Phosphorylation in the Absence and Presence of SR(RS2)

enzyme	[SR(RS2)] (nM)	k_{cat} (s^{-1})	K_{SR} (nM)
SRPK1	0	0.33 ± 0.04	30 ± 9
SRPK1	200	1.4 ± 0.20	28 ± 11
SRPK1(ΔN)	0	0.07 ± 0.02	63 ± 16
SRPK1(ΔN)	200	0.06 ± 0.01	72 ± 19
SRPK1(ΔS)	0	0.15 ± 0.02	26 ± 12
SRPK1(ΔS)	200	0.12 ± 0.01	25 ± 8
SRPK1(ΔS$_{INT}$)	0	0.40 ± 0.04	57 ± 20
SRPK1(ΔS$_{INT}$)	200	1.5 ± 0.13	66 ± 13
SRPK1(ΔSα1)	0	0.40 ± 0.04	48 ± 10
SRPK1(ΔSα1)	200	0.36 ± 0.03	55 ± 12

Although some RS domains contain long arginine−serine stretches (>6 repeats), others contain numerous, short stretches of four or fewer dipeptide repeats. How these diverse stretches are modified and what role they play in SR protein function is not well understood. In prior studies, we showed that the 50-residue RS domain of the prototype SR protein SRSF1 can be divided into two functional subdomains, RS1 and RS2 (Figure 1A). SRPK1 efficiently phosphorylates the eight arginine−serine repeats in RS1 driving SRSF1 into the nucleus for subsequent splicing function.[15,16] In the nucleus, the CLK kinases phosphorylate RS2 and alter subnuclear localization.[16] The strong preference of SRPK1 for RS1 over RS2 appears to be the result of the juxtaposition of a docking groove and active site that supports the stable binding and multisite phosphorylation of longer arginine−serine stretches[12,13] (Figure 1B). These findings now raise the question of whether some regions of an RS domain may be dispensable for the SRPK1 reaction. We addressed this issue for one SR protein SRSF1 and found that the nonconsensus region in its RS domain (RS2) is not a silent element with regard to SRPK phosphorylation as originally thought but rather plays an active role in controlling SRSF1 phosphorylation efficiency.

RS Domain Modulates ADP Release Rates through the NRF. Using a combination of deletion and charge-to-alanine mutations, we showed that the RS2 segment is important for facilitating SRSF1 phosphorylation by enhancing the rate of ADP release, the rate-limiting step for SR protein phosphorylation.[17] Interestingly, we also showed that the RS2 segment can be physically detached from the full RS domain and then used to activate a substrate form lacking these residues [SR(ΔRS2)]. This is consistent with a secondary binding site for RS2 that becomes engaged while RS1 is poised for phosphorylation in the active site of SRPK1. RS2-dependent activation is not due to effects on the cooperative binding of RS1 and RS2 but is due to an enhancement in maximum turnover. This suggests that RS2 exerts its effect by exclusively increasing the rate of ADP release. This modulatory phenomenon is entirely dependent on a functioning NRF composed of sequences outside the kinase domain. Such findings indicate that SRPK1 incorporates a structural relay switch that connects the RS domain and the nucleotide pocket.

NRF-RS Domain Interactions Enhance Phosphorylation Efficiency. The kinetic analyses presented herein indicate that surfaces outside the active site and docking groove of SRPK1 are important for SRSF1 phosphorylation. Presently, it is not certain whether RS2 directly encounters the NRF or whether it acts indirectly to modulate NRF function. The X-ray structure with SRSF1 bound lacks many portions of the RS

domain making it difficult to ascertain exactly its location on SRPK1. Nonetheless, given the expected proximities of the N-terminus, helix Sα1, and C-terminal sequences of the RS domain within the N-lobe (Figure 1B), RS2 may associate with the NRF and provide a direct route for SR protein phosphorylation enhancement through the modulation of nucleotide exchange rates (Figure 5). In such a mechanism,
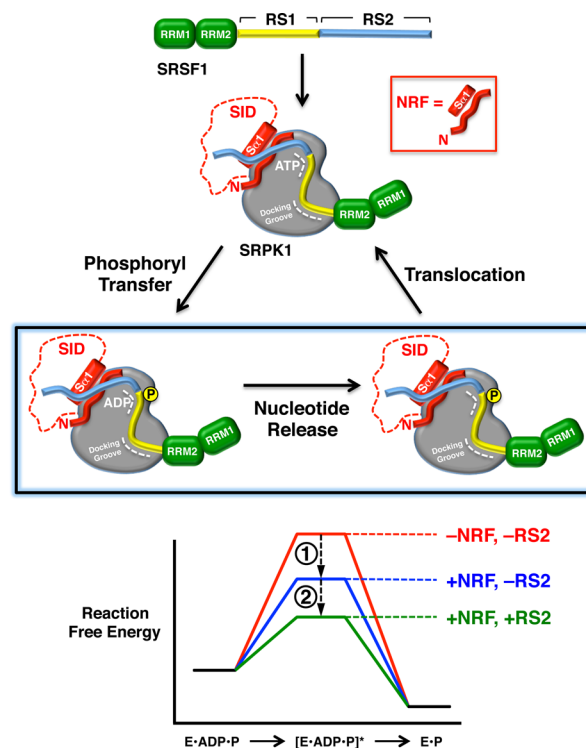

Figure 5. Model for RS2-dependent activation of SRPK1. The SRPK1−SRSF1 complex undergoes fast phosphoryl transfer followed by rate-limiting ADP dissociation (nucleotide release). Translocation reflects movement of the RS domain in the docking groove and active site and ATP binding for the delivery of subsequent phosphates. A 10-fold enhancement in net SR protein phosphorylation is achieved in a two-step process where step 1 involves a 3-fold increase resulting from the effect of the NRF on the nucleotide pocket and step 2 involves an additional 3-fold increase in ADP release resulting from NRF−RS2 modulatory interactions.

the rate of ADP release is modulated by two principal factors. First, the NRF provides a 3-fold, basal level of rate enhancement in the absence of RS2 (step 1; Figure 5). This value is known from the differences in k_{cat} for SR(ΔRS2) using SRPK1 and SRPK1(ΔN), a construct lacking a functioning NRF (Table 1). In a previous study we showed that k_{cat} for the full-length SRSF1 using SRPK1(ΔN) is the same as that for SR(ΔRS2) in the present study indicating that RS2 does not enhance ADP release without the NRF.[21] Second, the basal ADP release rate with the NRF is further enhanced by an additional 3-fold in the presence of RS2 and a functioning NRF (step 2; Figure 5). This value is estimated from a comparison of k_{cat} for SRSF1 and SR(ΔRS2) using SRPK1 (Table 1). Overall, these studies show that the net 10-fold increase in SR protein phosphorylation rate is the result of functional interactions between the NRF and RS2. Finally, it is possible that RS2 does not directly contact the NRF and binds at a different region in SRPK1. In this scenario, RS2 and the NRF might be allosterically related with no direct physical connection.

Regardless, whether RS2 interacts directly or indirectly with the NRF, the data presented herein indicate that a functioning NRF is necessary for RS2-dependent activation of SRPK1.

CONCLUSIONS

SR proteins represent a group of 12 essential factors that regulate alternative gene splicing.[3] Although SRPKs phosphorylate these factors and control splice-site choice, there is still no clear understanding of their substrate specificities and how various parts of the SR protein interact with the kinase and regulate phosphorylation levels. In a prior study, we showed that a structural module outside the kinase domain of SRPK1 increases the phosphorylation rate of the prototype SR protein SRSF1 by regulating ADP release rates.[21] We now show that sequences within the RS domain that are not part of the immediate consensus sequence and not considered important for SRPK1-directed subcellular control play an important role in regulating this module. We showed that the RS2 segment in SRSF1 interacts either directly or indirectly with the NRF. While the NRF is capable of increasing RS1 phosphorylation by a basal level, the RS2 segment further enhances this reaction (Figure 5). These studies identify a "molecular trigger" that links RS domain sequences with nucleotide exchange and raises the possibility that other SR proteins with larger, more complex RS domains may cause NRF-dependent changes in ADP release.

ASSOCIATED CONTENT

Ⓢ Supporting Information

MALDI-TOF spectra of SR protein substrates in the absence and presence of SRPK1 and ATP. This material is available free of charge via the Internet at http://pubs.acs.org.

AUTHOR INFORMATION

Corresponding Author
*Joseph A. Adams. Tel: 858-822-3360. Fax: 858-822-3361. E-mail: j2adams@ucsd.edu.

Notes
The authors declare no competing financial interest.

ABBREVIATIONS

ESE, exonic splicing enhancer; $C_{AT}T_{RAP}$, catalytic trapping; NRF, nucleotide release factor; RRM, RNA recognition motif; RS domain, domain rich in arginine−serine repeats; SID, spacer insert domain; SR protein, splicing factor containing arginine−serine repeats; SRPK1, SR-specific protein kinase 1; SRSF1, SR protein splicing factor 1 (aka ASF/SF2)

REFERENCES

(1) Zhou, Z., Licklider, L. J., Gygi, S. P., and Reed, R. (2002) Comprehensive proteomic analysis of the human spliceosome. *Nature* 419 (6903), 182−185.

(2) Stojdl, D. F., and Bell, J. C. (1999) SR protein kinases: The splice of life. *Biochem Cell Biol.* 77 (4), 293−298.

(3) Manley, J. L., and Krainer, A. R. (2010) A rational nomenclature for serine/arginine-rich protein splicing factors (SR proteins). *Genes Dev.* 24 (11), 1073−1074.

(4) Kataoka, N., Bachorik, J. L., and Dreyfuss, G. (1999) Transportin-SR, a nuclear import receptor for SR proteins. *J. Cell Biol.* 145 (6), 1145−1152.

(5) Lai, M. C., Lin, R. I., Huang, S. Y., Tsai, C. W., and Tarn, W. Y. (2000) A human importin-beta family protein, transportin-SR2, interacts with the phosphorylated RS domain of SR proteins. *J. Biol. Chem.* 275 (11), 7950−7957.

(6) Mathew, R., et al. (2008) Phosphorylation of human PRP28 by SRPK2 is required for integration of the U4/U6-U5 tri-snRNP into the spliceosome. *Nat. Struct. Mol. Biol.* 15 (5), 435−443.

(7) Wu, J. Y., and Maniatis, T. (1993) Specific interactions between proteins implicated in splice site selection and regulated alternative splicing. *Cell* 75 (6), 1061−1070.

(8) Kohtz, J. D., et al. (1994) Protein-protein interactions and 5′-splice-site recognition in mammalian mRNA precursors. *Nature* 368 (6467), 119−124.

(9) Zhou, Z., et al. (2012) The Akt-SRPK-SR axis constitutes a major pathway in transducing EGF signaling to regulate alternative splicing in the nucleus. *Mol. Cell* 47 (3), 422−433.

(10) Chalfant, C. E., et al. (2002) De novo ceramide regulates the alternative splicing of caspase 9 and Bcl-x in A549 lung adenocarcinoma cells. Dependence on protein phosphatase-1. *J. Biol. Chem.* 277 (15), 12587−12595.

(11) Sumanasekera, C., et al. (2012) C6 pyridinium ceramide influences alternative pre-mRNA splicing by inhibiting protein phosphatase-1. *Nucleic Acids Res.* 40 (9), 4025−4039.

(12) Ma, C. T., Hagopian, J. C., Ghosh, G., Fu, X. D., and Adams, J. A. (2009) Regiospecific phosphorylation control of the SR protein ASF/SF2 by SRPK1. *J. Mol. Biol.* 390 (4), 618−634.

(13) Ngo, J. C., et al. (2008) A sliding docking interaction is essential for sequential and processive phosphorylation of an SR protein by SRPK1. *Mol. Cell* 29 (5), 563−576.

(14) Ma, C. T., et al. (2008) Ordered multi-site phosphorylation of the splicing factor ASF/SF2 by SRPK1. *J. Mol. Biol.* 376 (1), 55−68.

(15) Velazquez-Dones, A., et al. (2005) Mass spectrometric and kinetic analysis of ASF/SF2 phosphorylation by SRPK1 and Clk/Sty. *J. Biol. Chem.* 280 (50), 41761−41768.

(16) Ngo, J. C., et al. (2005) Interplay between SRPK and Clk/Sty kinases in phosphorylation of the splicing factor ASF/SF2 is regulated by a docking motif in ASF/SF2. *Mol. Cell* 20 (1), 77−89.

(17) Aubol, B. E., and Adams, J. A. (2011) Applying the brakes to multisite SR protein phosphorylation: substrate-induced effects on the splicing kinase SRPK1. *Biochemistry* 50 (32), 6888−6900.

(18) Ding, J. H., et al. (2006) Regulated cellular partitioning of SR protein-specific kinases in mammalian cells. *Mol. Biol. Cell* 17 (2), 876−885.

(19) Zhong, X. Y., Ding, J. H., Adams, J. A., Ghosh, G., and Fu, X. D. (2009) Regulation of SR protein phosphorylation and alternative splicing by modulating kinetic interactions of SRPK1 with molecular chaperones. *Genes Dev.* 23 (4), 482−495.

(20) Plocinik, R. M., et al. (2011) Regulating SR protein phosphorylation through regions outside the kinase domain of SRPK1. *J. Mol. Biol.* 410 (1), 131−145.

(21) Aubol, B. E., Plocinik, R. M., McGlone, M. L., and Adams, J. A. (2012) Nucleotide release sequences in the protein kinase SRPK1 accelerate substrate phosphorylation. *Biochemistry* 51 (33), 6584−6594.

(22) Colwill, K., et al. (1996) SRPK1 and Clk/Sty protein kinases show distinct substrate specificities for serine/arginine-rich splicing factors. *J. Biol. Chem.* 271 (40), 24569−24575.

(23) Hagopian, J. C., et al. (2008) Adaptable molecular interactions guide phosphorylation of the SR protein ASF/SF2 by SRPK1. *J. Mol. Biol.* 382 (4), 894−909.

(24) Aubol, B. E., et al. (2003) Processive phosphorylation of alternative splicing factor/splicing factor 2. *Proc. Natl. Acad. Sci. U.S.A.* 100 (22), 12601−12606.

(25) Adams, J. A., and Taylor, S. S. (1992) Energetic limits of phosphotransfer in the catalytic subunit of cAMP- dependent protein kinase as measured by viscosity experiments. *Biochemistry* 31 (36), 8516−8522.

(26) Aubol, B. E., Nolen, B., Vu, D., Ghosh, G., and Adams, J. A. (2002) Mechanistic insights into Sky1p, a yeast homologue of the mammalian SR protein kinases. *Biochemistry 41* (31), 10002−10009.

(27) Zhou, J., and Adams, J. A. (1997) Participation of ADP dissociation in the rate-determining step in cAMP- dependent protein kinase. *Biochemistry 36* (50), 15733−15738.

(28) Waas, W. F., Rainey, M. A., Szafranska, A. E., and Dalby, K. N. (2003) Two rate-limiting steps in the kinetic mechanism of the serine/threonine specific protein kinase ERK2: A case of fast phosphorylation followed by fast product release. *Biochemistry 42* (42), 12273−12286.

(29) Kuzmic, P. (1996) Program DYNAFIT for the analysis of enzyme kinetic data: Application to HIV proteinase. *Anal. Biochem. 237* (2), 260−273.

(30) Aubol, B. E., et al. (2013) Partitioning RS domain phosphorylation in an SR protein through the CLK and SRPK protein kinases. *J. Mol. Biol. 425* (16), 2894−2909.